3

Radiation Sensitive Vacuum Electronic Components and Devices

J.A. Eichmeier

3.1 Historical Development

The fundamental phenomena, which make possible the function and application of this group of vacuum electronic components and devices, are the external photoelectric effect and secondary electron emission. Electromagnetic radiation with wavelengths in the range of infrared, visible light, ultraviolet or X-rays and particle radiation when hitting the surface of a metal, semiconductor or insulator in a vacuum tube cause the emission of electrons from this surface into the vacuum. By application of electric and/or magnetic fields within the tube, the electron current can be used:

1. for the detection of weak light signals with pulse durations down to the picosecond range and for the detection of particle-, UV- and X-radiation, respectively. In each case the input signals are transformed into small electrical current impulses with subsequent current amplification (secondary electron multipliers);
2. for the conversion and amplification of infrared, visible, ultraviolet or X-ray images into visible intensified light images (image converters, image amplifiers);
3. for the conversion of visible light pictures into electrical currents as input signals for television devices (television camera tubes).

The historical development of these types of radiation sensitive vacuum tubes is characterized by the following detections and inventions:

1887: H. Hertz observes that the ignition voltage of a spark gap decreases when the negative electrode is irradiated with UV light.

1888: W. Hallwachs shows that the effect detected by Hertz is caused by the emission of negatively charged particles from the negative electrode.

1890: J. Elster and H. Geitel, and also P. Lenard show that the charged particles are electrons. Elster and Geitel construct the first vacuum photocells for studying the photoeffect of alkali metals.

1902: L.W. Austin and H. Starke detect the secondary electron emission from metals.
1905: A. Einstein detects the energy equation of the photoelectric effect (Einstein equation).
1928: R. Suhrmann describes the photocurrent amplification by secondary electron emission and the principle of photomultipliers.
1929: V.K. Zworykin invents the first television camera tube (the Iconoscope).
1934: P. Farnsworth and G. Holst describe independently the principle of image converters and image amplifiers.
1950: P.K. Weimer et al. from RCA construct the first photoconductive camera tube (the Vidicon).

3.2 Electrophysical Fundamentals

The function of radiation sensitive vacuum electronic components described in this section is based on photoelectron emission, secondary emission, and electron optics.

3.2.1 Photoelectron Emission

Photons with wavelengths from infrared radiation down to X-rays incident on a solid surface (photocathode) cause the emission of photoelectrons according to the energy equation (Einstein equation)

$$E_\mathrm{k} = hf - W_\mathrm{c}, \tag{3.1}$$

where E_k is the kinetic energy of the emitted photoelectron, h is the Planck constant, f is the frequency of the photon and W_c is the work function of the photocathode. The smallest light frequency f_min or the largest wavelength $\lambda_\mathrm{max} = c/f_\mathrm{min}$ necessary for the emission of photoelectrons ($E_\mathrm{k} = 0$) is defined by

$$f_\mathrm{min} = W_\mathrm{c}/h \quad \text{or} \quad \lambda_\mathrm{max} = hc/W_\mathrm{c}. \tag{3.2}$$

λ_max is the cut-off wavelength of the photocathode. A monochromatic light flux Φ (in lumen, lm) of the frequency f is equal to a power flux Φ_e (in Watt, W) through a cross-section A,

$$\Phi_\mathrm{e} = S_\mathrm{ph} hf A, \tag{3.3}$$

where S_ph is the number of photons incident on the surface per second and cm^2. For the wavelength $\lambda = 555$ nm (maximum eye sensitivity), the relationship between Φ (in lm) and Φ_e (in Watt) is

$$1\ \mathrm{W} = 673\ \mathrm{lm}\ (\lambda = 555\ \mathrm{nm}) \quad \text{or} \quad 1\ \mathrm{lm} = 0.001484\ \mathrm{W}. \tag{3.4}$$

A part r of a light flux Φ_o incident on a solid surface is reflected (r is the reflection factor). The penetrating light flux Φ_a is given by

$$\Phi_a = \Phi_o(1 - r). \tag{3.5}$$

The penetrating light flux Φ_a is absorbed in the solid according to

$$\Phi_a = \Phi_o e^{-\alpha x}, \tag{3.6}$$

where α is the light absorption coefficient, x is the light pathlength in the solid and Φ_a is the light flux at x. For $x_o = 1$, we have $\Phi = \Phi_a$. x_o is called light penetration depth.

The photoelectron yield A_e of a photocathode is defined as the emitted photocurrent I_{ph} divided by the light power flux Φ_e,

$$A_e = I_{ph}/\Phi_e. \tag{3.7}$$

The lumen sensitivity s_c is defined as photocurrent per lumen

$$s_c = I_{ph}/\Phi, \tag{3.8}$$

and the quantum efficiency η_q as

$$\eta_q = S/S_{ph}, \tag{3.9}$$

i.e. the number S of photoelectrons emitted per incident photon. From (3.3) and (3.7)–(3.9) follows

$$\eta_q/\% = 0.124 A_e/(\text{mA/W})/\lambda/\mu\text{m}. \tag{3.10}$$

Semiconductors are preferred as light sensitive layers for photocathodes because of their low light reflection, high photon absorption coefficient, large emission depth and high quantum efficiency as compared with metals. The quantum efficiency, η_q, of different photocathodes as a function of photon energy, E_{ph}, and light wavelength, λ, respectively, is shown in Fig. 3.1. The points of intersection of these curves with the abscissa indicate the cut-off wavelengths of the photocathodes. Characteristic values of technically important photocathodes are presented in Table 3.1.

Table 3.1. Characteristics and applications of some photocathodes

Material	Nomenclature				Applications
	s_c (μA/lm)	A_e (mA/W)	η_q (%)	λ_{max} (μm)	
S-1/Ag-O-Cs	60	6	0.5	0.8	IR detectors
S-10/Bi-Ag-O-Cs	80	40	10	0.45	Camera tubes
S-11/Cs_3Sb on MnO	80	65	20	0.44	Multiplier, scintillation counters
S-20/(Cs)Na_2KSb	300	130	30	0.42	Image amplifiers, photometers, camera tubes

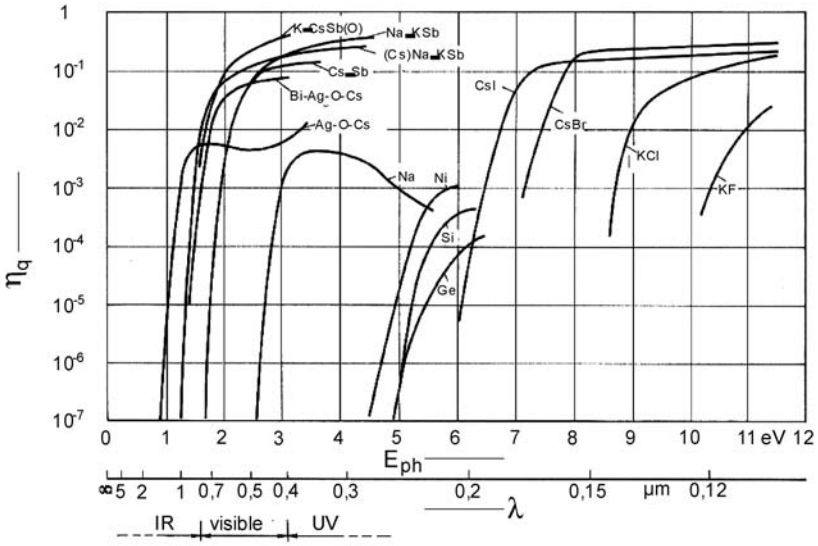

Fig. 3.1. Quantum efficiency, η_q, of different photocathodes as a function of photon energy, E_{ph}, and of the light wavelength, λ, respectively

3.2.2 Secondary Electron Emission

A primary electron beam with an energy of a few tens eV or more, incident on the surface of a solid, produces the emission of secondary electrons with a typical energy distribution, as shown in Fig. 3.2. The left maximum at low primary electron energy is due to "genuine" secondary electrons (share: 90%), the small right maximum represents elastically reflected primary electrons (about 3%) and the broad minimum is caused by backdiffused primary electrons (about 7%) which lost energy by many collisions with atoms of the solid. The thickness of the emission layer, from which most of the secondary electrons originate, is about 50 nm for metals and 500 nm for semiconductors and insulators, in which electron scattering is much smaller as compared with metals. The secondary electron current, I_s, depends on the primary current, I_{pr}, the primary electron energy, E_{pr}, and the angle of incidence of the primary ray. It depends also on the material and surface properties of the solid. The relationship between I_s and I_{pr} is given by

$$I_s = \delta I_{pr} \quad \text{or} \quad \delta = I_s / I_{pr}, \tag{3.11}$$

were δ is the secondary emission coefficient. The values of δ in dependence on the primary electron energy E_{pr} show maxima in the E_{pr}-range of some hundred eV (see Fig. 3.3). The maximum values δ_{max} are about 1 . . . 3 for metals and 3 . . . 20 for semiconductors and insulators.

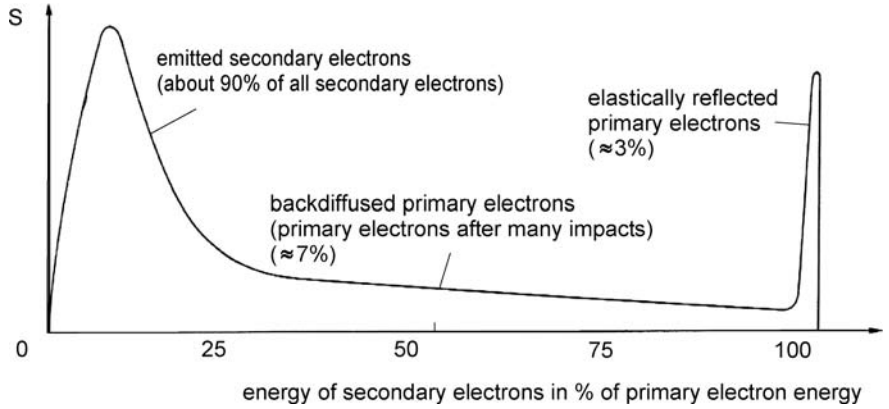

Fig. 3.2. Energy distribution of secondary electrons emitted from a solid (primary electron energy $E_{\mathrm{pr}} \approx 300 \ldots 1000$ eV)

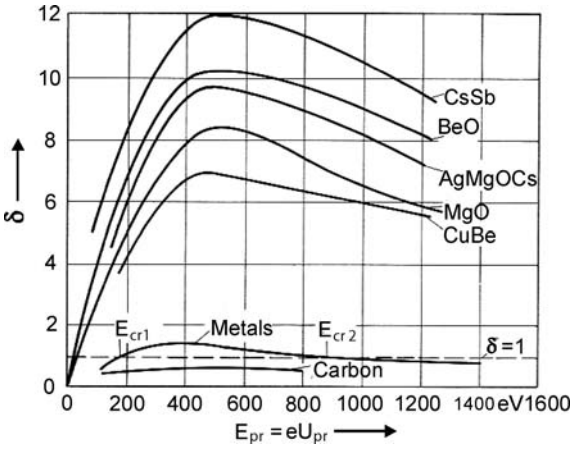

Fig. 3.3. Secondary emission coefficient, δ, as a function of the primary electron energy, E_{pr}, for different solids. $E_{\mathrm{cr1,2}}$ = crossover points for $\delta = 1$

3.2.3 Electron Optics

Electron optics deals with the quasi-optical behaviour of electron beams under the influence of electrical and magnetic fields in a vacuum system. For analogies and characteristic differences between geometrical light optics and electron optics, see [2].

Electric and magnetic electron lenses consist of electrically charged electrodes (aperture discs or cylinders) and current-carrying magnet coils, respectively, which produce electric or magnetic fields with spherically curved equipotential surfaces. Electric and magnetic deflection systems contain deflection electrodes and coils, re-

spectively, which produce flux lines perpendicular to the electron beam. Details on electron optics are discussed in [1–4].

3.3 Present State-of-the-Art and Applications

3.3.1 Secondary Electron Multipliers

Such vacuum tubes amplify a secondary electron current produced by electromagnetic or particle radiation incident on a sensitive entrance electrode. There are three types of multipliers (see Table 3.2).

Photomultipliers

Such vacuum tubes contain a photocathode and up to 12 electrodes (dynodes) for secondary electron emission. The surface of the dynodes consists of a material with high secondary emission coefficient δ. A voltage is applied to each dynode, which increases from the first to the last dynode by a constant amount. Consequently, the electron current from the photocathode is amplified at the first dynode and each of the following dynodes by a factor δ. The current amplification factor is given by

$$V_i = I_\mathrm{a}/I_\mathrm{o} = \delta^n, \tag{3.12}$$

where I_a is the anode current (current from the last electrode), I_o is the current from the photocathode, δ is the secondary emission coefficient of each dynode and n is the number of dynodes. In technical photomultiplier tubes, there is a loss of electrons between the photocathode and the first dynode (loss factor f) and between the dynodes (loss factor g). Considering these losses, (3.12) is to be replaced by

$$V_i = f(g\delta)^n. \tag{3.13}$$

Normally, the factor f amounts to about 0.9 and g to about 0.98. With

$$\delta = AU^a \tag{3.14}$$

Table 3.2. Types of secondary electron multipliers

Name	System	Type of radiation at the entrance
Photomultiplier	Photocathode + Electron multiplier system	IR-, UV- or visible light
Channel amplifier	Channel with resistive wall layer	α-, β-, γ-radiation, X- and UV-rays, fast ions and electrons
Scintillation counter	Scintillator + Photocathode + Electron multiplier system	α-, β-, γ- and X-rays

Table 3.3. Photocathode material, window material and spectral sensitivity range of modern photomultiplier tubes

Cathode material	Window material	Spectral sensitivity range/nm
Ag-O-Cs	Boron silicate glass	400 . . . 1200
CsSb	Boron silicate glass	185 . . . 650
Multialkali (Na-K-Sb-Cs)	Silica glass	185 . . . 930
CsTe	MgF_2	115 . . . 320

Equation (3.13) becomes

$$V_i = KU^{an}, \tag{3.15}$$

where A is a constant, K is a constant (containing f and g), U is the stage voltage defined as the voltage between two successive dynodes. The coefficient a is normally 0.7 . . . 0.8. According to (3.15), the current amplification factor V_i varies with the 6th to 10th power of U. The total supply voltage must therefore be highly stabilized. Its harmonic content and its temperature sensitivity must be very low.

The light entrance window of photomultipliers is either located on the side (side-on type) or on the front surface (head-on type) of the glass bulb. The side-on tubes have an opaque and the head-on ones a semitransparent photocathode, respectively. The spectral sensitivity range depends on the materials of the cathode and entrance window (see Table 3.3). The limit of sensitivity of photomultipliers is determined by the anode dark current and noise. The anode dark current increases with the supply voltage and with the temperature. The equivalent noise input is defined as the input power producing a signal-to-noise ratio equal to one at the output. It increases with the dark current, the current amplification factor and the signal band width. It decreases with a rising photosensitivity of the system.

Under the influence of a magnetic field of some mT the current amplification of photomultipliers is reduced by a factor of the order of 10 or more. The effect is especially high if the magnetic field is perpendicular to the system axis. It can be avoided by suitable shielding.

The dynamic behaviour of secondary electron multipliers, when irradiated with short light impulses, is governed by the electron transit time and the anode pulse rise time. Both values depend on the multiplier design and decrease with increasing supply voltage.

In Fig. 3.4 different commonly used types of photomultiplier tubes are shown. The tubes differ especially by the forms and positions of the dynodes. The surface of the dynodes consists of a layer of CuBe, AgMg, AlMg or $SbCs_3$ with values of $\delta \gg 1$. Characteristic data are: the voltage between each couple of dynodes is 150 to 280 V, the total voltage up to 3 kV, the current amplification $10^6 \ldots 10^8$, the sensitivity 10 . . . 60 mA/lm and the dark current 1 . . . 100 nA.

For the visualization of γ-ray pictures in Gamma cameras, position sensitive photomultipliers are applied. In such vacuum tubes the anode is, for instance, divided into 16 square fields. Each field has an area of $2.6 \times 2.6\,\text{mm}^2$ and a gap distance of 0.3 mm. An electron current, emitted from a definite point of the photocathode and

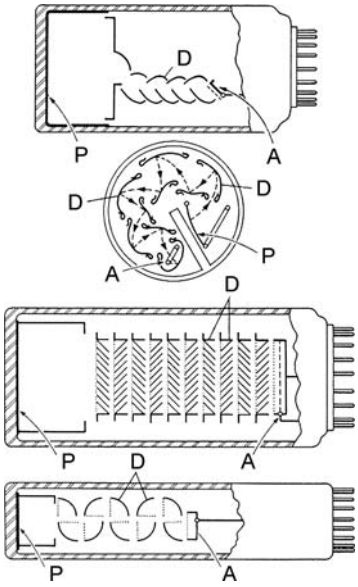

Fig. 3.4. Forms of commonly used types of photomultiplier cubes with different dynode forms. *P* is the photocathode, *A* is the anode and *D* denotes the dynodes

amplified by dynodes of the Venetian Blind type (3. tube in Fig. 3.4), hits one of the anode areas and produces an output signal. The space resolution depends primarily on the extension of the anode fields.

Channel Secondary Electron Multipliers

Channel multipliers contain – instead of single dynodes – a continuous dynode surface in the form of a resistive layer at the inner wall of a small straight, circular or spiral lead glass vacuum tube (Fig. 3.5). The length of the tube is a few centimeters and the inner diameter 1 . . . 2.5 mm. The active layer has a resistance of $10^9 \ldots 10^{11}$ Ohm and the necessary vacuum pressure within the tube is about 10^{-4} mbar. Between the two ends of the multiplier channel a direct voltage of 2 . . . 4 kV is applied (Fig. 3.6). An electromagnetic or particle radiation incident at the channel entrance causes the emission of secondary electrons from the resistive layer. The voltage drop across the layer accelerates the electrons in the direction of the outlet of the tube.

By successive impacts on the channel walls, the secondary electrons are multiplied generating an electron avalanche. The maximum current amplification is about 3×10^8. The channel tube can be used as an amplifier for currents as low as 1.6×10^{-19} A (open channel end) or as particle or quantum counter for maximum count rates of several $10^5\ s^{-1}$.

The current amplification as a function of the supply voltage of a channel multiplier is shown in Fig. 3.7. The upper limit of the amplification is caused by space charge effects. Channel multipliers show – when used as particle or quantum

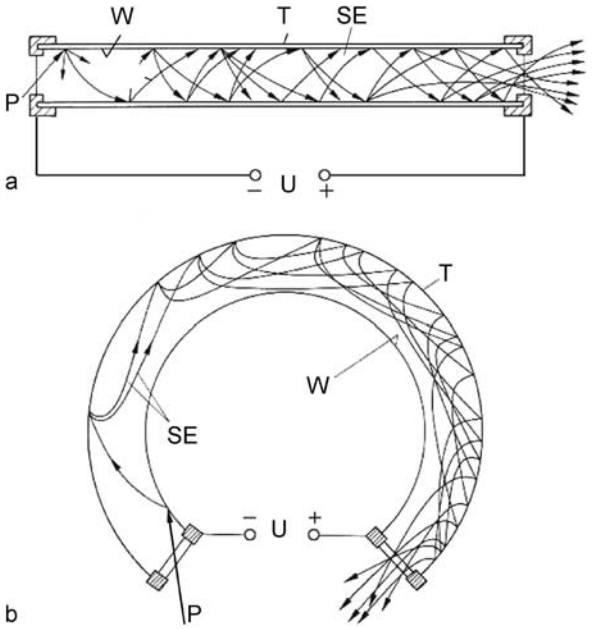

Fig. 3.5. Channel secondary electron multiplier with straight (**a**) and circular glass vacuum tube (**b**). *T* is the glass tube, *W* is the resistive wall, *P* is the incident particle or radiation, *SE* are the paths of secondary electrons and *U* is the supply voltage

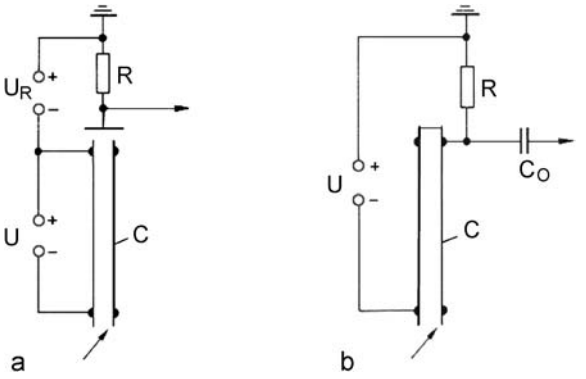

Fig. 3.6. Mode of operation of a channel multiplier with open (**a**) and closed outlet (**b**). *C* is the multiplier channel and *U* is the supply voltage

counters – a dependence of current amplification as a function of count rate. For small count rates ($1 \ldots 10^3\,\mathrm{s}^{-1}$), the amplification remains constant and then decreases with rising count rate.

Channel multipliers with an inner diameter greater than 0.5 mm are bent. This prevents penetration of positive residuous gas ions to the channel entrance, where

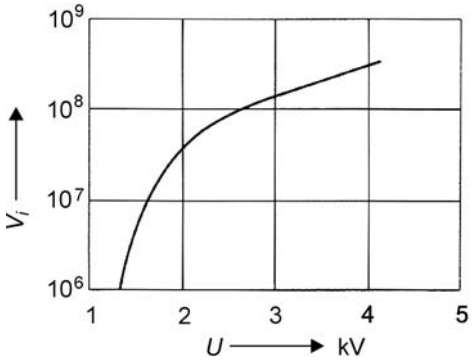

Fig. 3.7. Current amplification, V_i, as a function of the supply voltage, U, of a channel multiplier

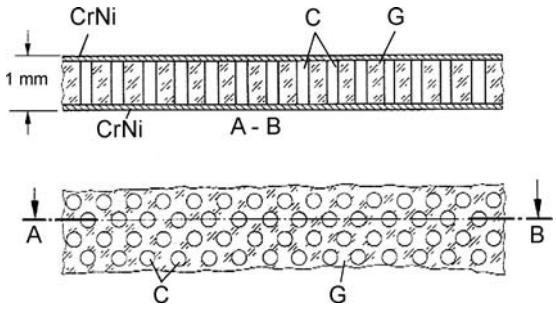

Fig. 3.8. Structure of a channel plate for the amplification of electron pictures. *G* is the glass plate, *C* is a single amplifying channel and *CrNi* is the CrNi-layer

they could release additional impulses. They are used as detectors for β-, UV- and X-rays, and also for positive and negative ions. Their impulse rise time is of the order of 5 ns, their half-amplitude pulse durations are about 10 ns and their noise count rate, for instance, $0.5\,s^{-1}$.

If a very large number of short multiplier channels (length about 1 mm) are placed in parallel and close together, a channel plate for the amplification of electron pictures is obtained (Fig. 3.8). Such secondary electron multiplier plates (diameter 2.5 . . . 10 cm) are produced by stringing, cutting and bunching of many tiny glass tubes with or without a solid core (of metal or soluble glass). The core is then chemically or electrolytically removed. Both sides of the channel plate are covered with evaporated chrome-nickel-layers. A voltage of 1 . . . 4 kV is applied between the layers. Each channel has a diameter of 25 . . . 50 µm and a wall resistance of $10^7 \ldots 10^8$ Ohm. The distance between two channel axes is 30 . . . 50 µm. The current amplification is about 10^3.

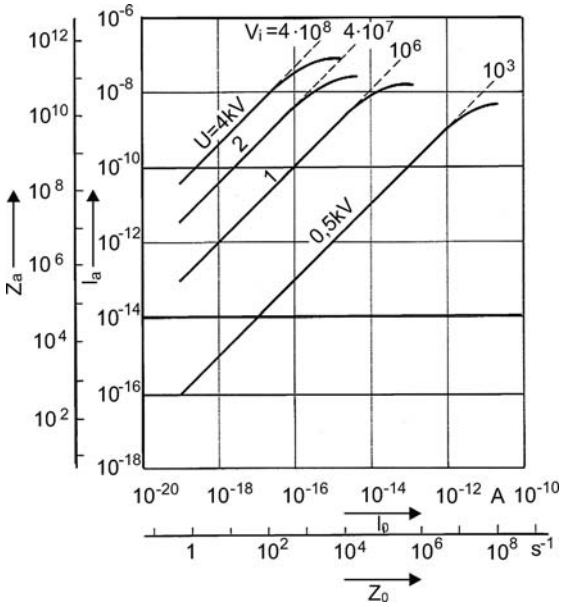

Fig. 3.9. Transfer characteristic of a channel plate (output current as a function of input current). I_0 is the input current, z_0 is the number of incident electrons per second, I_a is the output current, z_a is the number of emitted electrons per second, U is the supply voltage and V_i is the current amplification factor

The transfer characteristic of a channel plate (i.e. the output current as a function of the input current) is shown in Fig. 3.9. The structure of an ultra-fast photomultiplier with channel plate is illustrated in Fig. 3.10.

Scintillation Counters

Scintillation is defined as energy conversion of radioactive radiation into light impulses by means of a solid, liquid or gaseous medium. Commonly used inorganic scintillators are semiconductors like NaJ activated with Thallium, ZnS activated with Silver, or BGO (chemical structure: $Bi_4(GeO_4)_3$). An organic scintillator is, for instance, Anthracene. The activator atoms produce discrete energy levels in the forbidden band of the semiconductor. Particles or radiation quants of sufficient energy penetrating into the scintillation crystal cause the transition of valence electrons from the valence band to the activator energy levels. The following return of the electrons to the valence band is accompanied by the emission of photons similar to the light of a luminescent screen when irradiated with electrons. If the scintillation crystal is connected to the transparent cathode of a photomultiplier, the photons from the crystal produce photoelectron impulses from the cathode which are amplified and detected. The design of a scintillation counter with photomultiplier is shown in Fig. 3.11. The maximum pulse rate depends on the decay time of the scintillator impulses, which amounts to 1 . . . some 100 ns (Table 3.4).

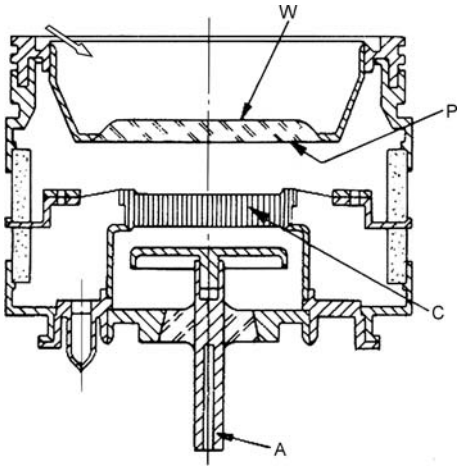

Fig. 3.10. Ultra-fast photomultiplier system with channel plate. *W* is the window, *P* is the photocathode, *C* is the channel plate and *A* is the anode

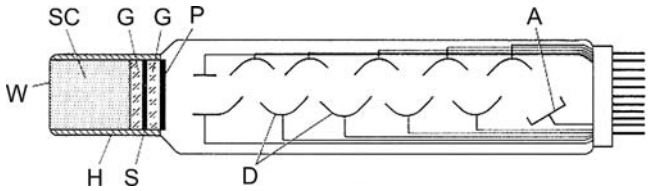

Fig. 3.11. Structure of a scintillation counter with photomultiplier. *W* is the radiation entrance window (for instance, 0.5 mm Al coated with a MgO-layer to reduce light reflection), *SC* is the scintillator crystal (for instance, NaJ(TI)), *H* is the air-tight case (because NaJ is strongly hygroscopic), *G* is the glass plate; *S* is the silicon layer, *P* is the photocathode; *D* is the dynode and *A* is the anode

Table 3.4. Parameters of different inorganic scintillation materials

	BGO $Bi_4(GeO_4)_3$	LSO $Lu_2(SiO_4)O$:Ce	NaJ(Tl)	BaF_2
Decay time/ ns	300	40	230	620
Absorption Length/ cm	1.12	1.14	2.56	2.06
Peak wavelength/ nm	480	420	410	310
Light yield relative to NaJ/ %	20	75	100	6

The particle or quantum energy, absorbed in the scintillator, is proportional to the amplitude of the emitted light impulse. A scintillation counter connected to a pulse height analyser can therefore be used for energy spectrometry of X-ray- and γ-quants.

3.3.2 Image Converters and Image Amplifiers

These types of vacuum tubes convert a weak light, X-ray- or γ-ray-picture into a bright visible picture. For this purpose, the light radiation containing the picture information is absorbed on the frontside of a transparent photocathode, which produces a photoelectron emission picture on its backside. The photoelectron picture is, by electron-optical means, projected to a fluorescent screen to make it visible. In the case of X- and γ-rays, the entrance of the image converter consists of a fluorescent layer (X-rays) and of a scintillator crystal (γ-rays), respectively, which convert the X- or γ-ray picture into a visible light picture on the subsequent photocathode [5].

Image Converters for Visible, Infrared or Ultraviolet Light Input Signals and for X-rays

The converters for light input signals can be divided into three different design groups (Fig. 3.12). Converter tubes of the proximity or wafer design (Fig. 3.12a) contain a plane photocathode and a plane luminescent screen at a small distance behind it (proximity structure). A short positive high voltage impulse on the screen produces a photoelectron current impulse and the corresponding short-time image of at least 1 ns duration. The projection is almost free of distortion and image inversion. The image amplification factor is about 20. Such tubes are applied as electrooptical high-speed shutters for photo cameras.

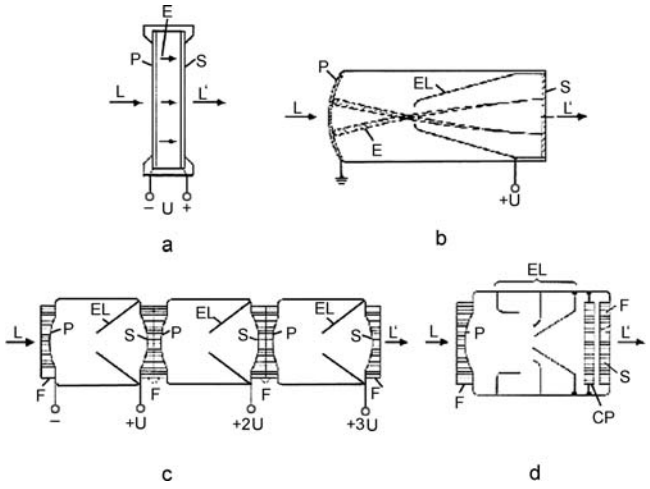

Fig. 3.12. Types of image converters for light input signals. **a** Proximity or wafer design. **b** Image amplifier with electrostatic lens. **c** Threestage image amplifier with fiberoptic coupling windows. **d** Image converter with a channel plate. *P* is the photocathode, *S* is the luminescent screen, *E* is the electron beam, *EL* is the electron lens, *F* is the fiberoptic window, *CP* is the channel plate, *L* is the incident light flux, L' is the amplified light flux and *U* is the supply voltage

In a second type of image amplifiers, an electrostatic lens is positioned between the photocathode and the screen (Fig. 3.12b) causing an image inversion on the screen. Such inverter image amplifiers have a light amplification factor of about 100 and a small image distortion. If several (normally three) image amplifier units are connected in series and coupled through fiberoptic windows to each other, a multistage image amplifier with a maximum amplification factor of 75,000 is obtained (Fig. 3.12c). A fiberoptic window consists of a very large number of fine, short and parallel positioned glass fibers which transfer the screen image of one stage to the immediately following photocathode of the next stage.

A third group of image converters belongs to the inverter type tubes containing a channel plate for additional electron multiplication between the electrostatic lens and the screen (Fig. 3.12d). The lens projects the electron image of the photocathode onto the front surface of the channel plate. The electrons leaving the channel plate are accelerated to the screen where they produce a visible bright image. The light amplification factor of such tubes depends on the channel plate voltage. Channel plates show a saturation of their transfer characteristic for increasing input currents, i.e. for stronger irradiation of the photocathode. This makes possible the amplification of images with high contrast.

The resolving power of image converters is defined as the maximum number of clearly separated line pairs per millimeter. It is limited by the fact that each point on the photocathode, when electrooptically projected on the screen, produces a tiny disc of distortion. Image converters with lens systems have a higher resolving power as compared with tubes which have no focusing lens.

Vacuum image converters are operating with a high screen voltage (maximum 15 kV) resulting in a high image brightness and small chromatic and spherical aberrations. In tubes with large diameter, the photocathode is bent to minimize scale errors. Typical parameters of converter tubes are: cathode diameter 20 . . . 50 mm, cathode sensitivity $s_c = 50 \ldots 200\ \mu A/lm$ at a wavelength $\lambda = 550$ nm, light amplification factor $20 \ldots 5 \times 10^4$, scale of image enlargement 0.6 . . . 1.5, resolving power

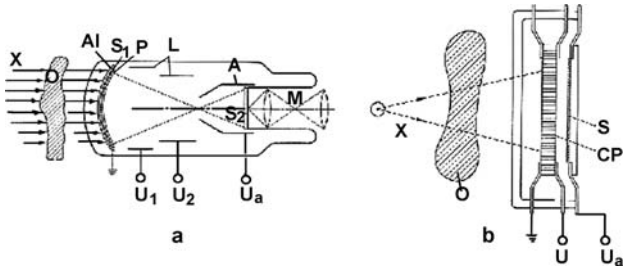

Fig. 3.13. Structures of X-ray image amplifiers. **a** Tube with one photocathode and two luminescent screens. **b** Tube with channel plate and one luminescent screen. *X* denotes X-rays, *O* is the irradiated object, *Al* is the aluminum foil, *S*, S_1, S_2 are the screens, *P* is the photocathode, *L* is the electron lens, *A* is the anode, *M* is the microscope, *CP* is the channel plate, U_a is the accelerating voltage and *U* is the voltage at the channel plate

10 . . . 60 line pairs/mm and background brightness $<2 \times 10^{-7}$ Lux (caused by the dark current).

A special type of vacuum image converters are X-ray-image amplifiers (Fig. 3.13), which transform a weak X-ray image into a bright visible picture. The tube in Fig. 3.13a contains a photocathode and two luminescent screens. The first (entrance) screen S_1 is irradiated by the X-rays and produces a light picture on the adjacent photocathode P. This photocathode emits the corresponding electron picture which is projected onto the second screen S_2 by an electron lens L. The final image is transferred to a television monitor tube. In the X-ray image amplifier of Fig. 3.13b the electron-optical system consisting of the screen S_1, the photocathode P and the electron lens L is replaced by a channel plate CP in front of a luminescent screen S. The channel plate transforms the incident X-ray image into a bright visible image on the screen. Vacuum X-ray image amplifiers are to a large extent applied in medical diagnostics and in material structure analysis.

Gamma Cameras

A radioactive, γ-quants emitting isotope, when injected into the organism, takes part – like the non-radioactive isotopes of the same element – in all transport, metabolic and secretion processes of this organism. Because of its γ-radiation, the isotope can serve as an indicator or tracer, the path and concentration of which can be tracked within the organism (first application by G. von Hevešy on plants, 1913).

Within the organism the isotope traverses under the influence of metabolic processes one or more compartments (organs or part of organs), where it can at first be temporarily accumulated to form a pool before it is secreted. By detecting and measuring the corresponding variations of the organism emitted γ-radiation, the activity distribution in time and space can be analysed. Thus, information about the function and volume of the compartments and also about the flow and exchange rates between the compartments can be obtained. The pictures showing the spatial distribution of the γ-radiation within the organism are picked up with a scintillation or γ-camera (Anger camera).

The design and mode of operation of a scintillation camera is shown in Fig. 3.14. The γ-radiation emitted from the body of a patient penetrates a perforated collimator with a large number of tiny holes (for instance, diameter 39 000 holes of length 30 mm and diameter 1.6 mm; perforation pitch 0.25 mm). At the outlet of the collimator the radiation hits on a scintillation crystal with diameter of 20 . . . 30 cm and thickness of 6 . . . 12 mm. The scintillator can consist of a single piece of crystal (for instance NaJ) or of a large number of small crystals, each of which is shielded against the radiation of each neighbour crystal. The crystal surface opposite to the collimator is covered with a large number (about 20 . . . 100) of tightly packed small photomultipliers. The locations of the scintillation points within the single crystal sensor are detected by means of a decoding matrix (resistance matrix after Anger or delay line matrix after Tanaka). In such a matrix the distance between a scintillation point and a reference point is proportional to the resistance or to the signal transit time

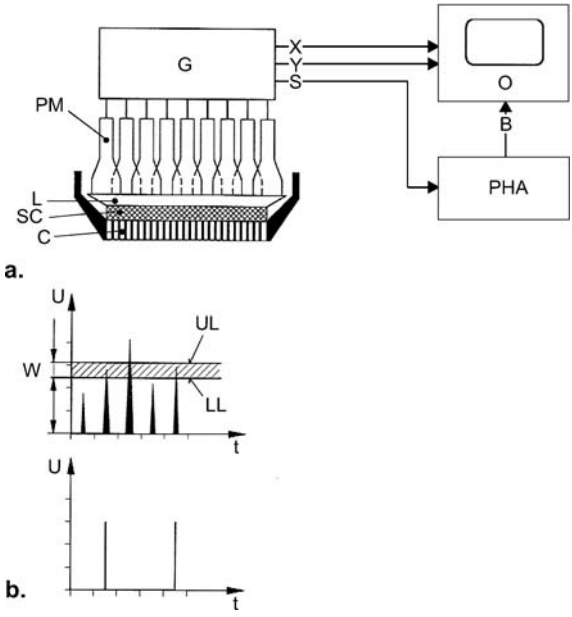

Fig. 3.14. Design and mode of operation of a scintillation camera (Gamma camera). **a** Block diagram, **b** Energy window of the pulse height analyser. *PM* is the photomultiplier array, *L* is the light conductor, *SC* is the scintillation crystal, *C* is the collimator, *G* is the generator for coordinate and sum impulses, respectively; x, y are deflection signals, *S* is the sum impulse, *O* is the oscilloscope, *B* is the brightness control, *PHA* is the pulse height analyser, *W* is the channel width, *UL*, *LL* is the upper and lower channel limit, t is the time, U is the signal voltage

between these points. The output signal amplitudes of the photomultipliers are proportional to the energy of the γ-quants. The influence of the γ-quantum energy can be eliminated through division of the impulse amplitudes by the amplitude of the summary impulse (Z-impulse). The Z-impulses are conveyed to the input of a pulse height analyser (two parallel analysers with different thresholds in anti-coincidence). This circuit separates within a definite energy window impulses originating from the characteristic γ-energy of a single nuclid and suppresses the Compton radiation of low energy. Therewith, the energetic separation of two γ-emitters in double nuclid studies is possible. The output impulses of the pulse height analyser modulate the brightness of the pixels on the screen. The brightness distribution corresponds to the γ-activity distribution of the body region of interest. This mapping is suitable for γ-quants within the energy range of 100 . . . 600 keV.

The scintigrams can continuously – in cardiological investigations synchronously with the electrocardiogram – be stored in a computer. In this way, for instance, changes of the function of organs in "regions of interest"can be detected and volume measurements of organs are possible.

Typical characteristics of Gamma cameras are: the sensitivity, i.e. the number of detected γ-quants divided by the number of emitted γ-quants; the resolving power, i.e. the half-amplitude pulse duration divided by the quantum energy in percent; the spatial resolution (for instance 1.8 mm); the homogeneity, i.e. the constancy of sensitivity across the scintillator surface; and the linearity and time resolution (for instance 2×10^5 impulses/s). Modern Gamma cameras contain microprocessors for homogeneity and energy correction.

3.3.3 Television Camera Tubes

This group of vacuum tubes is used for the conversion of visible light, infrared and UV images into electrical output signals (videosignals) [5].

Basic Function of Vacuum Camera Tubes

A modern camera tube consists of four principal components (see Fig. 3.15): a light sensitive converter target at the entrance of the tube, an electron beam system, a beam focusing system and a beam deflecting system.

The Converter Target

The photosensitive target of a modern vacuum camera tube is composed of a glass substrate of optical quality (window) covered with two subsequent layers: a highly transparent electrically conductive layer (signal electrode) and a photo-sensitive layer, generally consisting of several semiconducting substances. The properties of the semiconducting layers determine essentially the characteristics of the camera tube.

Three types of semiconducting targets are mainly used, namely the photoconductive resistance target, the single junction diode target and the silicon multidiode target.

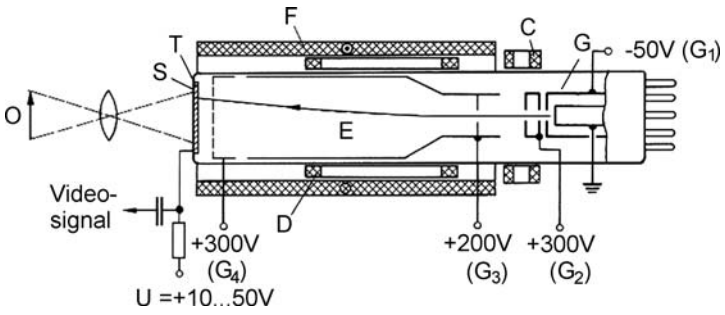

Fig. 3.15. Basic design of a Vidicon. *O* is the optical object, *S* is the signal plate, *T* is the target, *F* is the focusing coil, *D* are deflecting coils, *C* is the correction coil, *G* is the electron gun, *E* is the scanning electron beam

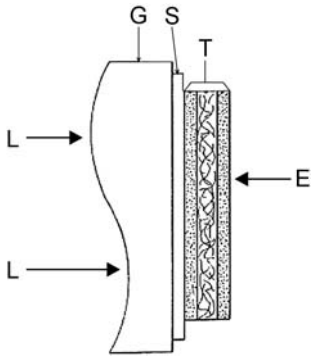

Fig. 3.16. Basic structure of the Vidicon target. *L* is the incident light flux, *G* is the glass window, *S* is the signal layer, *T* is the target layer, *E* is the scanning electron beam

The basic structure of the Vidicon target is shown in Fig. 3.16. The transparent signal electrode layer consists of indium tin oxide (ITO) or tin oxide doped with antimon (SnO_x(Sb)) and the target layer of three subsequent films of compact, porous and again compact semiconducting antimontrisulfide (Sb_2S_3). The films also differ in their stoichiometric composition and thickness.

In the case of single junction diode targets, the glass substrate is covered with a transparent ITO- or SnO_x(Sb)-signal electrode followed by several layers of amorphous or polycrytalline semiconducting materials forming a junction barrier. The semiconductor of the Plumbicon target (Fig. 3.16) is composed of subsequent n-, i- and p-conductive microcrystalline lead oxide layers with a junction barrier located in the intrinsic (i) zone. The semiconducting material of the Newvicon target is a ZnSe-film covered with In-doped ZnCdTe- and Sb_2S_3-films, forming a heterojunction within the semiconductor. The photosensitive layer of the silicon multidiode target (Fig. 3.17) is a silicon monocrystal with a light exposed and highly doped thin n^+-Si-layer followed by a normally doped n-Si-layer. On the surface of the n-Si-layer, $(6 \ldots 8) \times 10^5$ planar diodes per cm^2 are integrated by planar diffusion. Each diode has a diameter of $6 \ldots 8$ µm and a mid-distance of $12 \ldots 15$ µm.

The different types of photosensitive targets of vacuum camera tubes convert the optical image projected onto the frontside of the target into the corresponding electrical charge distribution across the backside. In the case of the photoconductive resistance target (Vidicon target; Fig. 3.16), the photons penetrate the thin signal layer and produce a spatial conductivity distribution across the subsequent semiconducting layer. A positive bias voltage at the signal electrode causes a transport of positive charge carriers from the signal electrode through the semiconducting layer to the open surface of this layer, where they accumulate. At each point the number of flowing and accumulating charge carriers depends on the electrical conductivity at this point. Thus a definite surface charge distribution corresponding to the photon distribution of the optical image is generated on the open surface of the target. During operation of the camera tube the charge distribution is continuously scanned and thus detected by a fine electron beam produced by an electron gun within the tube.

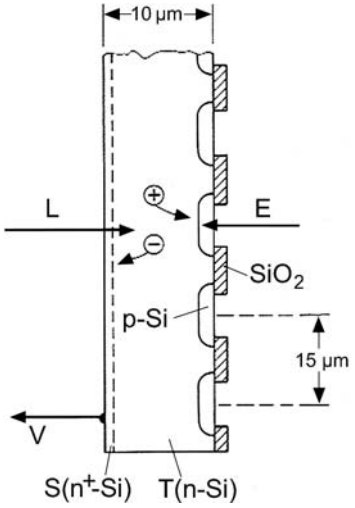

Fig. 3.17. Structure of the silicon multidiode target. *L* is the incident light flux, *S* is the signal layer, *T* is the target layer (n-Si with integrated p-Si-spots), *V* is the videosignal

In a single junction diode and multidiode target (Figs. 3.16 and 3.17) a reverse bias voltage is applied to each diode. In darkness only a very small and usually negligible reverse current is flowing over the barrier layer. Illumination of the target and consequently of the barrier layer produces electron-hole-pairs which are continuously separated by the reverse electrical field within the barrier zone. In this way the p-zone (or p-zones in the multidiode target) are positively charged. At each point of the single junction diode and in the p-zone of each diode in the multidiode target, respectively, the accumulated charge is proportional to the number of incident photons, i.e. the light intensity. This charge distribution can also be scanned by an electron beam.

The Electron Beam System

This system consists of the electron gun and the drift space. The gun can be a triode, a diode or a modified diode (Fig. 3.18).

The drift space of the electron beam system contains a cylindrical electrode connected to a grid electrode in front of and parallel to the target surface (Fig. 3.15). Both electrodes form an electrostatic lens (collimator lens) causing the electron paths to be perpendicular when the electrons hit the target surface.

The Beam Focusing and Deflecting Systems

The beam focusing and deflecting systems are magnetic coils positioned outside the vacuum tube. The focusing coil generates a homogeneous axial magnetic field along the electron beam. Electrons with additional radial velocity components are forced

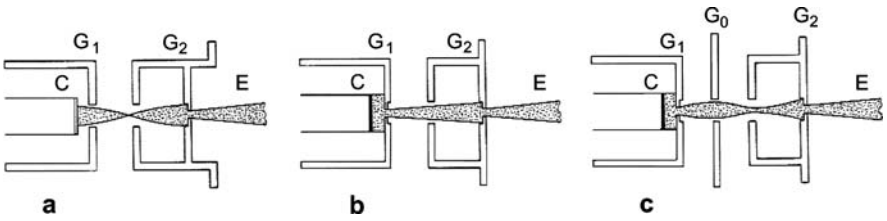

Fig. 3.18. Construction of typical electron guns for Vidicons. **a** Triode system. **b** Diode system. **c** Modified diode system. C is the thermionic cathode, G; G_1; G_2 are the beam forming electrodes, E is the electron beam

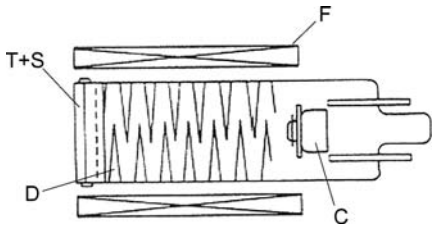

Fig. 3.19. Schematic design of a Vidicon system with magnetic beam focusing and electrostatic beam deflection. T+S is the transparent signal plate (S) with target layer (T), F is the focusing coil, D are deflecting electrodes, C is the cathode

to move on small circular paths and thus focused in one or several beam nodes. The accelerating voltage is adjusted so that the first beam node lies in the target surface.

The deflecting system consists of two pairs of coils for horizontal and vertical deflection. The coils are attached to the tube bulb and surround the bulb in the form of half-circles. The two pairs of coils have an angular displacement of 90 degrees. The application of a sweep voltage produces an alternating saw-tooth current with linear wave front and consequently two orthogonal magnetic deflecting fields. The frequencies correspond to the line and picture frequencies of the actual television standard.

The interference between the focusing and deflecting fields can be eliminated in tubes with electrostatic deflection and magnetic focusing. In this case the horizontal and vertical deflecting fields are generated by two zigzag-shaped electrode pairs (*Deflectron*, Fig. 3.19). Their forms and positions are adjusted to minimize picture defects. They are produced by evaporating a metallic layer on the inner wall of the bulb and subsequent computer-controlled laser structuring. The deflecting voltage of several hundred volts must be extremely linear and free of noise.

Mechanism of the Videosignal Production in Vacuum Camera Tubes

It has already been described above that the optical image at the entrance window of the camera tube produces an electrical charge distribution on the inner open surface of the semiconducting target layer. During operation of the tube, this charge distribution is continuously scanned with a fine and slow electron beam. The scanning

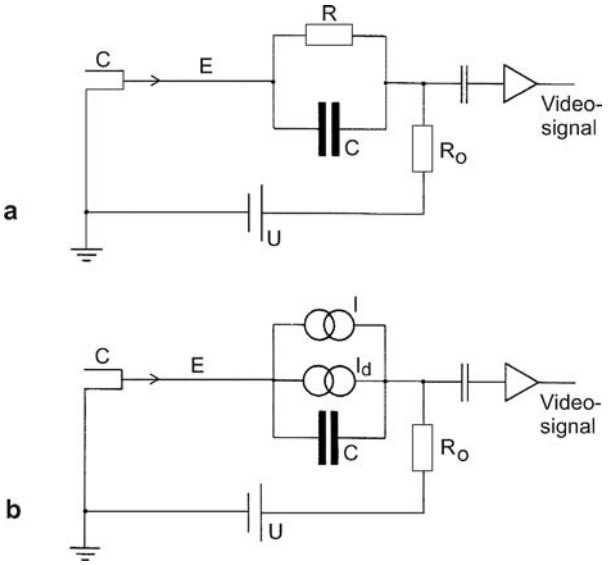

Fig. 3.20. Equivalent circuit diagram of an image point on the target. **a** Target with resistance layer. **b** Target with junction layer. *C* is the cathode, *E* is the scanning electron beam, *R*, *C* are resistance and capacitance of an image point, *I*, I_d are currents through an image point, U is the bias voltage across the target

process produces secondary electrons which are absorbed by the grid electrode in front of the target. Because the secondary electron coefficient is smaller than one, more primary electrons are absorbed than secondary electrons emitted. The positive charge distribution on the target surface is therefore partly or completely compensated by the scanning electron beam.

The effect of the scanning process can be described by means of the equivalent circuit of a single picture point of the target (Fig. 3.20). The diameter of each picture point is determined by the diameter of the scanning electron beam. For the photoconductive resistance target each picture point can be described as shunt connection of a high-ohm resistor *R* and a small capacitor *C* (Fig. 3.20a). In the case of the barrier junction target the equivalent circuit contains two current generators connected in parallel and a small capacitor (Fig. 3.20b). The capacitors are normally charged to the target potential (potential of the signal electrode).

During the scanning process, each picture point is hit by beam electrons within a very short time interval of about 0.1 μs. In this interval each point becomes part of the electronic circuit, in which the electron beam acts as fast switch. Without illumination the capacitors discharge to some extent between two subsequent scanning events. Through the next following scan this loss of charge is compensated. The corresponding current is the dark current of the camera tube. The voltage drop at the resistor R_o is the videosignal in darkness.

If an optical picture is projected on the (now illuminated) target, free movable electron-hole pairs are knocked off by the photons in the semiconducting target layer. Under the influence of the applied electrical field the charge carriers are separated. The free electrons move to the positive electrode (signal plate) and the holes to the negative electrode, i.e. to the open target surface which is stabilized at zero potential by the scanning electron beam. On the target surface the resulting instantaneous distribution of the positive charge density is equivalent to the light image at the tube entrance.

Between two subsequent scanning events the capacitors in Fig. 3.20 discharge. The discharge current, which is different for each image point, flows through the resistor, R, and current source, I, which are connected parallel to the capacitors, C. During the next scanning event, the charge loss of the capacitors is almost compensated. The corresponding compensation current produces a voltage drop across the resistor R_o, which is the videosignal of the tube. The series of voltage impulses with different amplitudes, generated during a frame period of the television system, contains the complete information of the television image. During the line and frame flyback, respectively, the target scanning is suppressed by negative blanking pulses on the control electrode or positive blanking pulses on the cathode of the electron gun.

Special Vacuum Electronic Camera Tubes

The *Ebsicon*: The light sensitivity of a Vidicon with silicon multidiode target can be increased by a factor of about 300 if an image amplifier is connected to the tube entrance (Fig. 3.21). In this case the target is not directly illuminated but bombarded with electrons from the image amplifier. The electron image emitted from the photocathode of the amplifier is projected on the silicon target producing a corresponding charge picture on the target surface. This type of camera tube is called Ebsicon (Ebsi = ***e***lectron ***b***ombarded ***si***licon).

The *Pyroelectric Vidicon* (Fig. 3.22): This type of camera tube is sensitive to infrared radiation. Its target is a thin dielectric disc of Triglycinsulfate (TGS) which is spontaneously polarized perpendicular to the surface. The tube entrance consists of

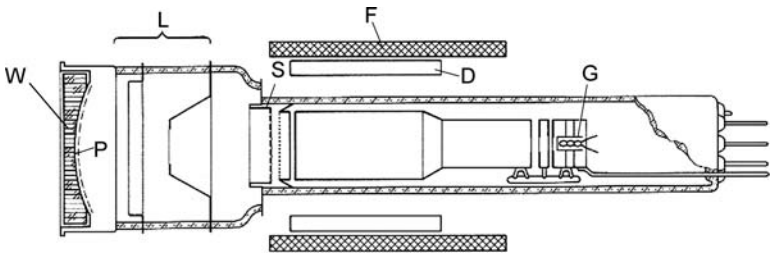

Fig. 3.21. Design of an Ebsicon (electron bombarded Si-Vidicon). *W* is the fiberoptic window, *P* is the photocathode, *L* is the electron lens system, *S* is the silicon target, *F* is the focusing coil, *D* are deflecting coils, *G* is the electron gun

a Germanium window. Incident IR-radiation, varying with time, changes the spatial temperature distribution and hence the polarization of the pyroelectric target layer. Consequently, the surface charge distribution on the target backside is also changed, whereas the illuminated frontside is kept on the constant positive potential of the adjacent signal plate. As the polarization is influenced only by variations of the IR-radiation, the radiation must be modulated through an optical chopper or by periodic movements of the camera with the result that the constant background radiation of an object has no effect and the weak contrast of a thermal scene is enhanced.

The scanned surface of the TGS-layer can have a positive or negative charge surface depending on the changes of polarization. For the electron beam scanning, it is necessary to increase the surface potential by a constant positive amount. For this purpose, the scanned surface is charged continuously with positive ions, which are generated by impacts of beam electrons on residual gas molecules near the target surface. The necessary gas pressure of Helium or Hydrogen gas is about 10^{-3} mbar. Another possibility is the production of positive surface charges by secondary emission or making the TGS-layer weakly conductive. The scanning beam diminishes the surface charge until each image point attains the cathode potential. The corresponding potential jumps yield the videosignal at the signal plate. The spectral sensitivity curve of a pyroelectric camera tube is shown in Fig. 3.23.

The optical resolution of an IR-camera tube is restricted by the thermal conductivity of the target, because the temperature profile produced by the IR-radiation is rapidly dissolving. An increasing modulation frequency causes a rising spatial resolution, but a decrease of the videosignal. For improvement of the image resolution targets with surface channel graticules are used. The channel distances are about 25 μm. The channel structure is made by ion etching with photomask technique.

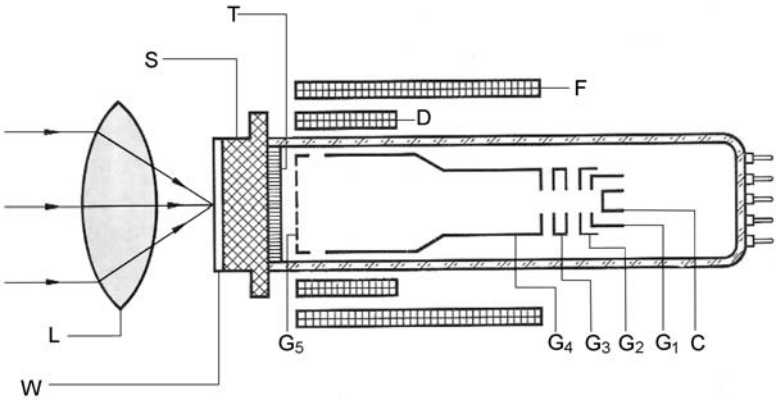

Fig. 3.22. Schematic design of a pyroelectric camera tube. *L* is the infrared lens, *W* is the IR-light window, *S* is the signal electrode, *T* is the pyroelectric target, *F* is the focusing coil, *D* are deflecting coils, *C* is the cathode, $G_{1...5}$ are the beam forming electrodes

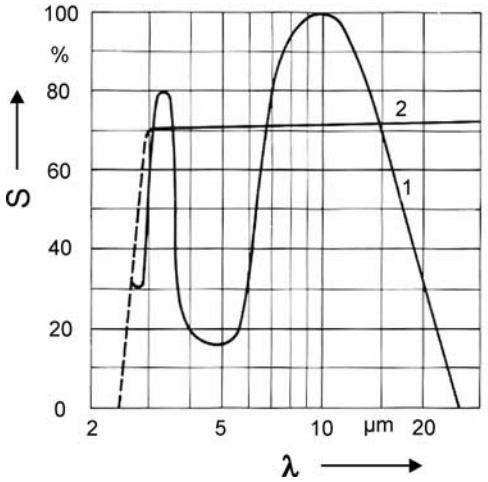

Fig. 3.23. Spectral sensitivity of pyroelectric Vidicons with different IR-entrance windows. *1* Germanium window. *2* Special IRTRAN-window. *S* is the spectral sensitivity (maximum = 100%), λ is the IR-wavelength

Geiger–Mueller Counter

Such tubes are used for intensity measurements of radioactive radiation. They consist of a glass or metal tube containing a cylindrical or spiral cathode and a straight axial metal filament as anode (Fig. 3.24). The tube is filled with gas of about 100 mbar. The gas consists of air, hydrogen or noble gases, with additional components of organic or inorganic vapours.

With increasing anode voltage U_a the following discharge processes take place in the counter tube (Fig. 3.25):

Low U_a (up to about 300 V): No formation of charge carrier avalanches (*Ionization Chamber Mode*).

Medium U_a (up to about 500 V): Formation of charge carrier avalanches on the path of incident radiation (spot of primary ionization); the discharge current is proportional to U_a and to the energy of the incident radiation (*Proportional Mode*);

High U_a (up to about 800 V): By intensive production of photons each incident particle or quant causes a "transverse ignition" of a discharge along the whole anode wire. The discharge current is not dependent on the energy of the particles or quants (*Geiger–Mueller Mode*). A further increase of U_a leads to a continuous glow discharge.

A quick extinction of each single discharge impulse can be achieved by using a RC-circuit for the tube operation (with large R and small C; see Fig. 3.24) and by addition of vapour components to the fill-gas, which cause a high absorption of photons (*self-quenching counting tube*). Because of the slow decay of the ion space charge GM-tubes show a definite *dead-time* after each discharge impulse

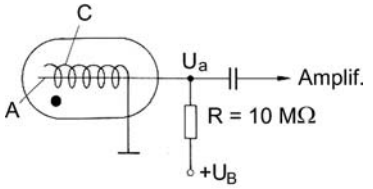

Fig. 3.24. Design and principal circuit of a Geiger–Mueller counter tube. *C* is the cathode (helix), *A* is the anode (straight wire), *U* is the supply voltage

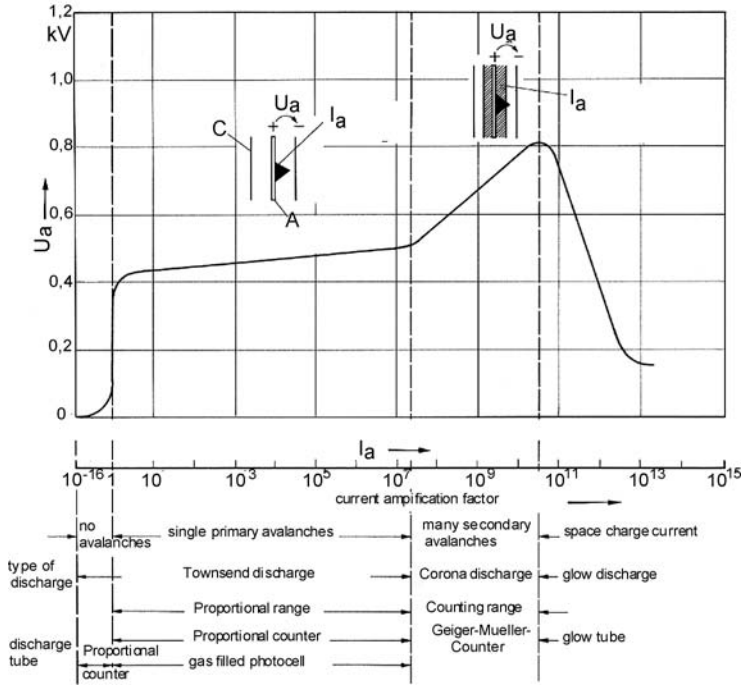

Fig. 3.25. Voltage-current-characteristic (U–I characteristic) of a Geiger–Mueller counter tube. Under the *abscissa* the different ranges of operation are shown

(0.01 . . . 1 ms; no response), followed by a *recovery time* (0.1 . . . 1 ms; weak response).

The pulse rate characteristic of a GM-tube, i.e. the pulse rate as a function of the anode voltage U_a, is shown in Fig. 3.26. The height of the plateau in the characteristic is proportional to the incident ion dose rate j.

Ionization Chamber

Ionization chambers are sensors for ion dose rate measurements. The glass or metal chamber contains two plane or cylindrical electrodes and is filled with pure air or

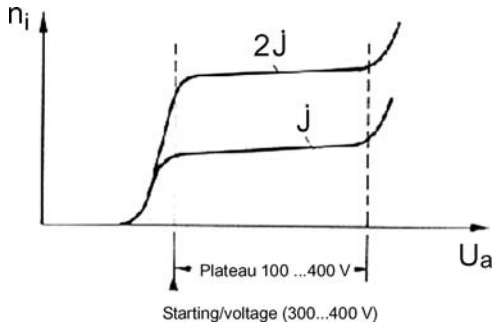

Fig. 3.26. Pulse rate characteristic of a Geiger–Mueller counter tube. n_i is the number of discharge impulses per second, U is the anode voltage, j is the ion dose rate

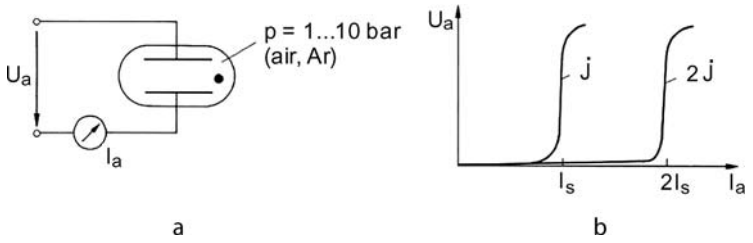

Fig. 3.27. Circuit (**a**) and U–I characteristic (**b**) of an ionization chamber. j is the ion dose rate, I is the saturation current

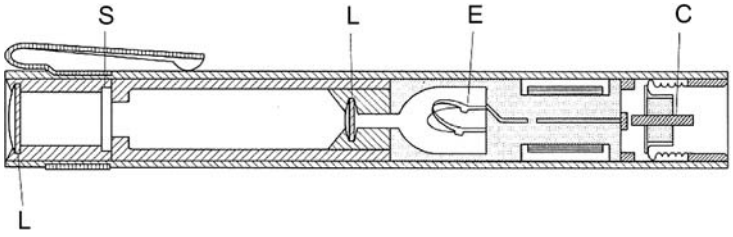

Fig. 3.28. Cross-section of a pocket dosimeter for radiology and nuclear technology. E is the quartz filament electrometer, L is the microscope lens, S is the scale, C is the contact pin for recharge

argon gas at atmospheric or a higher pressure. Therefore, strictly speaking, it does not belong to the group of vacuum tubes, but its production needs vacuum technology. The principal circuit of operation and the characteristic are shown in Fig. 3.27. The ion dose rate is defined as the charge of ions of one polarity produced in air in 1 s by the incident radiation. The saturation current (order of magnitude several pA) flowing between the electrodes is proportional to the ion dose rate. Ionization chambers are widely used as pocket dosimeters in radiology and nuclear engineering.

The dosimeter in Fig. 3.28 contains an electrically charged quartz filament, which is continuously discharged by the incident radiation. Such dosimeters have measur-

ing ranges between 5×10^{-5} and 0.15 C/kg ($0.2 \ldots 600\,R$; 1 R = 1 Roentgen = 2.58×10^{-4} C/kg).

3.4 Future Aspects of Radiation Sensitive Vacuum Electronic Components

Photomultiplier tubes, channel amplifiers and scintillation counters have – as compared with the corresponding semiconductor components – a very high light or radiation sensitivity, a large signal amplification factor and a fast response. Consequently, they are and will be used in a wide field of applications, e.g. for the detection of weak and short radiation impulses in physics and medicine.

A new development for future applications is the flat panel photomultiplier tube with an effective sensitive area of about $50 \times 50\,\text{mm}^2$ and a thickness of only 28 mm. When used in a matrix arrangement, the dead space between the tubes is extremely small, and the effective area becomes almost 90%. Each tube contains 12 dynodes and a 8×8 multianode matrix structure for spatial resolution detection. The anode pixel size is $5.8 \times 5.8\,\text{mm}^2$ and the spectral response range 300 ... 650 nm. Tubes of this type are, for example, used in Gamma cameras, Cherenkov counters and mammography units.

For photon counting in the near infrared (NIR) region (wavelength 950 ... 1400 nm), thermoelectrically cooled photomultiplier modules with integrated controller and vacuum pump have been developed. The tube has a fast time response (rise time 900 ps) and a high gain (about 10^6). Typical applications are photoluminescence, Raman spectrometry, cathodoluminescence, fluorescence and LIDAR.

Present and future applications of photo- and secondary electron multiplier tubes, described in this section, are, for example, spectrophotometers for UV-, IR- and visible light, spectrophotometers for atomic absorption, photoelectric emission, fluorescence or Raman scattering measurements for quantitative analysis of elements contained in a sample. Other spectrophotometric applications are liquid or gas chromatography, X-ray diffractometry, X-ray fluorescence analysis and electron microscopy. In semiconductor industry, narrow scanning beams of electrons, ions, light or X-rays are used to prove the quality of semiconductor surface structures, the secondary particles or rays being measured with electron multipliers or microchannel plates. For pollution monitoring, photomultipliers are used in atmospheric dust counters, turbulence meters for liquids, NO_x- and SO_x-meters. In biotechnology, electron multiplier tubes are, for instance, used in flow cytometers for biological cell counting and in DNA sequencers. In medicine, various types of scintillation counters are found in gamma cameras, positron computer tomography and liquid scintillation counting.

During the last decade image converters and television camera tubes have been partly and continuously replaced by equivalent semiconductor components. Vacuum tubes for these applications have the advantage of high sensitivity, high resolution, fast response and insensitivity against radioactive and cosmic radiation. Such properties are important in special fields like X-ray, infrared and gamma ray imaging. Consequently, it can be expected that vacuum image converter and television camera tubes will also play a considerable role in the near future.

References

[1] J. Bretting, *Technische Röhren* (Hüthig, Heidelberg, 1991)
[2] J. Eichmeier, *Moderne Vakuumelektronik* (Springer, Berlin, Heidelberg, New York, 1981)
[3] J. Eichmeier, H. Heynisch, *Handbuch der Vakuumelektronik* (Oldenbourg, München, Wien, 1989)
[4] Hamamatsu Report, *Photomultiplier Tubes* (2002)
[5] R. Steinbrecher, *Bildverarbeitung in der Praxis* (Oldenbourg, München, Wien, 1993)